

## THERMOCHEMICAL ABLATION OF CARBON/CARBON COMPOSITES WITH NON-LINEAR THERMAL CONDUCTIVITY

by

**Wei-Jie LI, Hai-Ming HUANG\*, and Yu-Meng HU**

Institute of Engineering Mechanics, Beijing Jiaotong University, Beijing, China

Original scientific paper  
DOI: 10.2298/TSCI1405625L

*Carbon/carbon composites have been typically used to protect a rocket nozzle from high temperature oxidizing gas. Based on the Fourier's law of heat conduction and the oxidizing ablation mechanism, the ablation model with non-linear thermal conductivity for a rocket nozzle is established in order to simulate the one-dimensional thermochemical ablation rate on the surface and the temperature distributions by using a written computer code. As the presented results indicate, the thermochemical ablation rate of a solid rocket nozzle calculated by using actual thermal conductivity, which is a function of temperature, is higher than that by a constant thermal conductivity, so the effect of thermal conductivity on the ablation rate of a solid rocket nozzle made of carbon/carbon composites cannot be neglected.*

Key words: oxidizing ablation, non-linear thermal conductivity, rocket nozzle, carbon/carbon composites

### Introduction

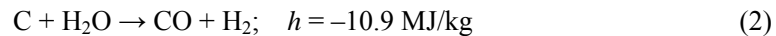
Carbon/carbon (C/C) composites combine lightweight, exceptional strength and stiffness, making them the material of choice for severe-environment applications. C/C composites can serve as thermal protection systems in a rocket nozzle subjected to the oxidizing gas such as CO<sub>2</sub>, and H<sub>2</sub>O at a high temperature [1]. Oxidation ablation of C/C composites may occur on the surface under a high temperature condition [2], and its rate is related to the gas components and pressure [3]. In the past 10 years, the heat balance integral method or moment integral method had been used for quasi-steady ablation [4, 5]. Some researchers kept their eyes on experimental aspects by using plasma guns, arc heater or scanning electron microscopy [6, 7], and the thermal behavior was simulated on the basis of Fourier's law and the ablation mechanism [8]. In order to simplify the calculation, many researchers took thermal conductivity as a constant instead of a function of temperature. This hypothesis may introduce some errors, *e. g.* Huang *et al.* [9] took a thermal conductivity as a function of temperature to make sure the error for the sublimation rate of C/C composites. However, there has been rare research on oxidizing ablation with a non-linear thermal conductivity. Based on the Fourier heat conduction law and the oxidizing ablation mechanism, we will analyze the effect of thermal conductivity on the ablation rate of a solid rocket nozzle made of C/C composites.

### Ablation model and numerical approach

The oxidizing gases at a high temperature flow through a nozzle, which is mainly combined of CO<sub>2</sub> and H<sub>2</sub>O. The oxidizing reaction is the ablation mechanism of a solid rocket nozzle made of C/C composites, and the thermochemical reaction are:

---

\* Corresponding author; e-mail: hmhuang@bjtu.edu.cn



where  $h$  is the absorbing heat of reaction. According to the Arrhenius law, the mass ablation rate of carbon can be obtained:

$$\dot{m}_c = \dot{m}_{c(\text{H}_2\text{O})} + \dot{m}_{c(\text{CO}_2)} \quad (3)$$

in which:

$$\dot{m}_{c(\text{H}_2\text{O})} = 0.0247 \frac{M_C}{M_{\text{H}_2\text{O}}} \exp\left(-\frac{E_0}{RT_w}\right) P_{\text{H}_2\text{O}} \quad (4)$$

$$\dot{m}_{c(\text{CO}_2)} = 0.0247 \frac{M_C}{M_{\text{CO}_2}} \exp\left(-\frac{E_0}{RT_w}\right) P_{\text{CO}_2} \quad (5)$$

where  $E_0 = 175.142 \text{ kJ/mol}$ ,  $R = 8.314472 \text{ J/mol}$ ,  $\dot{m}_c$  is the mass ablation rate of C/C composites,  $M$  – the relative molecular weight,  $T_w$  – the surface temperature, and  $P$  – the partial pressure; the subscripts C,  $\text{H}_2\text{O}$ ,  $\text{CO}_2$  are carbon,  $\text{H}_2\text{O}$  and  $\text{CO}_2$ , respectively.

From eq. (5), we can gain the line ablation rate vertical to the internal surface of a nozzle:

$$v = \frac{\dot{m}_c}{\rho} \quad (6)$$

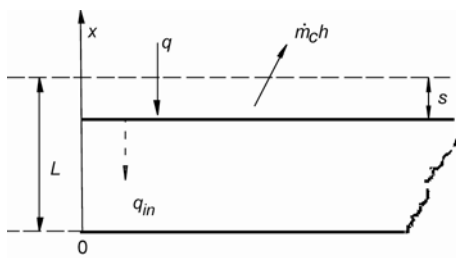


Figure 1. One-dimensional ablation model

where  $v$  and  $\rho$  are the line ablation rate and the density of C/C composites, respectively.

Because the temperature gradient vertical to the internal surface of a nozzle is much higher than that in the other orientations, the one-dimensional ablation model is built in fig. 1.

In the above model,  $L$  is the thickness of C/C composites plate,  $s$  is the ablation thickness, which is a function of time, and  $q_{in}$  is the heat flux entering the surface of material.

$$q_{in} = -k(T) \frac{\partial T(x,t)}{\partial x} \Big|_{x=L-s} \quad (7)$$

If thermal conductivity  $k(T)$  is a function of temperature, the one-dimensional heat conduction equation can be deduced on the base of the Fourier's law of heat conduction:

$$\rho c \frac{\partial T(x,t)}{\partial t} = k(T) \frac{\partial^2 T(x,t)}{\partial x^2} + \frac{\partial k(T)}{\partial T} \left[ \frac{\partial T(x,t)}{\partial x} \right]^2 \quad (8)$$

According to the model in fig. 1, the boundary conditions are given in the form:

$$-k(T) \frac{\partial T(x,t)}{\partial x} = q - \rho v h \quad x = L - s \quad (9)$$

$$\frac{\partial T(x,t)}{\partial x} = 0 \quad x = 0 \quad (10)$$

The initial condition is:

$$T(x,0) = T_0 \quad 0 \leq x \leq L \quad (11)$$

The heat conduction equations are obviously transient so that we have to discrete space domain and time domain, respectively. Here we use the central difference format for space domain and implicit format for time domain as:

$$\frac{\partial T(x,t)}{\partial x} = \frac{T_{j+1}^n - T_{j-1}^n}{2\Delta x} \quad (12)$$

$$\frac{\partial T^2(x,t)}{\partial x^2} = \frac{T_{j+1}^n - 2T_j^n + T_{j-1}^n}{\Delta x^2} \quad (13)$$

$$\frac{\partial T(x,t)}{\partial t} = \frac{T_j^n - T_j^{n-1}}{\Delta t} \quad (14)$$

Let  $A = [k(T)]/\rho c$ ,  $B = [\partial k(T)]/\partial T \cdot [\partial T(x, t)]/\partial x$ , and substituting  $A$  and  $B$  into eq. (8), we get:

$$\frac{\partial T(x,t)}{\partial t} = A \frac{\partial^2 T(x,t)}{\partial x^2} + B \frac{\partial T(x,t)}{\partial x} \quad (15)$$

With the help of eqs. (12), (13), and (14), from eq. (15) it is easy to obtain the discrete equation by using the Thomas algorithm:

$$\frac{T_j^n - T_j^{n-1}}{dt} = A \frac{T_{j+1}^n - 2T_j^n + T_{j-1}^n}{\Delta x^2} + B \frac{T_{j+1}^n - T_{j-1}^n}{2\Delta x} \quad (16)$$

Let  $G = A dt/\Delta x^2$ ,  $D = B dt/2\Delta x$ , and substituting  $G, D$  into eq. (16), we get:

$$T_j^n = \frac{G + D}{(1 + 2G) - (G - D)F_{j-1}} T_{j+1}^n + \frac{(G - D)Q_{j-1} + T_j^{n-1}}{(1 + 2G) - (G - D)F_{j-1}} \quad (17)$$

where

$$F_j = \frac{G + D}{(1 + 2G) - (G - D)F_{j-1}}, \quad Q_j = \frac{(G - D)Q_{j-1} + T_j^{n-1}}{(1 + 2G) - (G - D)F_{j-1}}$$

The discrete eq. (17) can be solved by using the chasing method, and the computational scheme is presented in fig. 2.

Based on the computational scheme, a computer code can be written for the sake of calculating the thermal response.

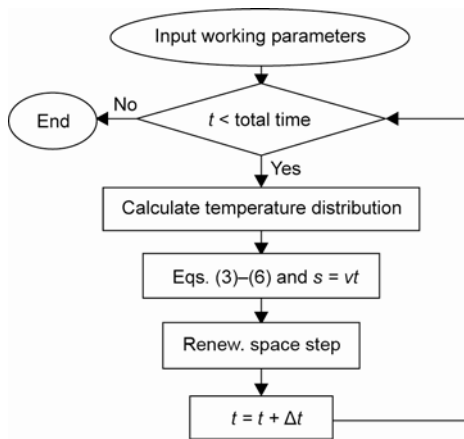


Figure 2. The computational scheme

Table 1. Working parameters

$L$ [mm]	$q$ [ $\text{Wm}^{-2}$ ]	$T_0$ [K]	$\rho$ [ $\text{kgm}^{-3}$ ]	$c$ [ $\text{Jkg}^{-1}\text{K}^{-1}$ ]
100	$6 \cdot 10^6$	300	2000	1870

It is assumed that the volume fraction of  $\text{H}_2\text{O}$  and  $\text{CO}_2$  in a nozzle is the equivalent percentage of 45%, and working parameters of C/C composites are shown in tab. 1.

Using parameters given in tab 1, we can obtain the thermal behavior of C/C composites plate by the written code. Figure 3 displays the bottom temperature of C/C composites plate at different heating times. Within the initial heating 60 s, the bottom temperature by a constant  $k$  rises slower than that by a function  $k(T)$ . However, when the heating time exceeds 120 s, the bottom temperature by a function  $k(T)$  begins to exceed that by a constant  $k$ .

Figure 4 indicates the ablative surface temperature of the C/C composites plate at different heating times. If  $k$  is constant surface temperature rises slower than if  $k$  is function of temperature. At the initial heating time, surface temperature in both cases rise abruptly, while rising slowly along with time. The ablative surface temperature for a constant  $k$  or function  $k(T)$  reaches a plateau, but the maximum relative error is 23.2% at 19.4 s.

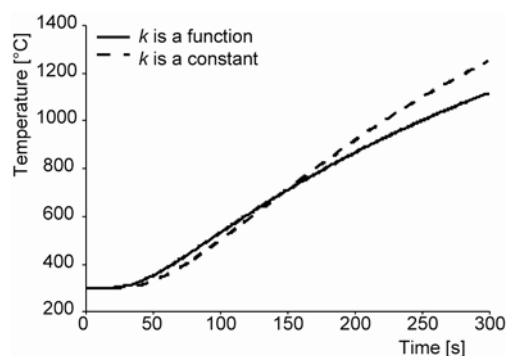


Figure 3. Bottom temperatures vs. time

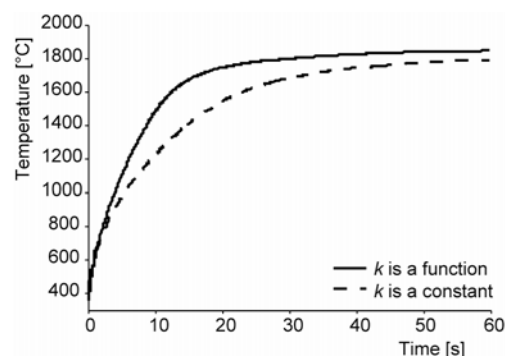


Figure 4. Surface temperatures vs. time

The line ablation rate of C/C composites plate within 60 s is shown in fig. 5. The line ablation rate by a constant  $k$  rises slower than that by a function  $k(T)$ . At the initial heating time, they all stay at 0 mm/s before 8 s. The line ablation rate by a function  $k(T)$  begins to rise at 8 s, while the line ablation rate by a constant  $k$  begins to rise at 19 s. The line ablation rate for  $k = k(T)$  is always higher than the other, and the maximum relative error is 67.2% at 42.8 s.

## Numerical results

In order to obtain the effect of thermal conductivity on the ablation rate, we respectively take a thermal conductivity as  $k = 70 \text{ Wm}^{-1}\text{K}^{-1}$  and a actual thermal conductivity as:

$$k(T) = 33.2 + 54.88 \cdot \exp\left[-\frac{T(x,t) - 300}{770}\right] \text{ [Wm}^{-1}\text{K}^{-1}] \quad (18)$$

It is assumed that the volume fraction of  $\text{H}_2\text{O}$  and  $\text{CO}_2$  in a nozzle is the equivalent percentage of 45%, and working parameters of C/C composites are shown in tab. 1.

Using parameters given in tab 1, we can obtain the thermal behavior of C/C composites plate by the written code. Figure 3 displays the bottom temperature of C/C composites plate at different heating times. Within the initial heating 60 s, the bottom temperature by a constant  $k$  rises slower than that by a function  $k(T)$ . However, when the heating time exceeds 120 s, the bottom temperature by a function  $k(T)$  begins to exceed that by a constant  $k$ .

Using parameters given in tab 1, we can obtain the thermal behavior of C/C composites plate by the written code. Figure 3 displays the bottom temperature of C/C composites plate at different heating times. Within the initial heating 60 s, the bottom temperature by a constant  $k$  rises slower than that by a function  $k(T)$ . However, when the heating time exceeds 120 s, the bottom temperature by a function  $k(T)$  begins to exceed that by a constant  $k$ .

Using parameters given in tab 1, we can obtain the thermal behavior of C/C composites plate by the written code. Figure 3 displays the bottom temperature of C/C composites plate at different heating times. Within the initial heating 60 s, the bottom temperature by a constant  $k$  rises slower than that by a function  $k(T)$ . However, when the heating time exceeds 120 s, the bottom temperature by a function  $k(T)$  begins to exceed that by a constant  $k$ .

Using parameters given in tab 1, we can obtain the thermal behavior of C/C composites plate by the written code. Figure 3 displays the bottom temperature of C/C composites plate at different heating times. Within the initial heating 60 s, the bottom temperature by a constant  $k$  rises slower than that by a function  $k(T)$ . However, when the heating time exceeds 120 s, the bottom temperature by a function  $k(T)$  begins to exceed that by a constant  $k$ .

Using parameters given in tab 1, we can obtain the thermal behavior of C/C composites plate by the written code. Figure 3 displays the bottom temperature of C/C composites plate at different heating times. Within the initial heating 60 s, the bottom temperature by a constant  $k$  rises slower than that by a function  $k(T)$ . However, when the heating time exceeds 120 s, the bottom temperature by a function  $k(T)$  begins to exceed that by a constant  $k$ .

Using parameters given in tab 1, we can obtain the thermal behavior of C/C composites plate by the written code. Figure 3 displays the bottom temperature of C/C composites plate at different heating times. Within the initial heating 60 s, the bottom temperature by a constant  $k$  rises slower than that by a function  $k(T)$ . However, when the heating time exceeds 120 s, the bottom temperature by a function  $k(T)$  begins to exceed that by a constant  $k$ .

Using parameters given in tab 1, we can obtain the thermal behavior of C/C composites plate by the written code. Figure 3 displays the bottom temperature of C/C composites plate at different heating times. Within the initial heating 60 s, the bottom temperature by a constant  $k$  rises slower than that by a function  $k(T)$ . However, when the heating time exceeds 120 s, the bottom temperature by a function  $k(T)$  begins to exceed that by a constant  $k$ .

Using parameters given in tab 1, we can obtain the thermal behavior of C/C composites plate by the written code. Figure 3 displays the bottom temperature of C/C composites plate at different heating times. Within the initial heating 60 s, the bottom temperature by a constant  $k$  rises slower than that by a function  $k(T)$ . However, when the heating time exceeds 120 s, the bottom temperature by a function  $k(T)$  begins to exceed that by a constant  $k$ .

Using parameters given in tab 1, we can obtain the thermal behavior of C/C composites plate by the written code. Figure 3 displays the bottom temperature of C/C composites plate at different heating times. Within the initial heating 60 s, the bottom temperature by a constant  $k$  rises slower than that by a function  $k(T)$ . However, when the heating time exceeds 120 s, the bottom temperature by a function  $k(T)$  begins to exceed that by a constant  $k$ .

Using parameters given in tab 1, we can obtain the thermal behavior of C/C composites plate by the written code. Figure 3 displays the bottom temperature of C/C composites plate at different heating times. Within the initial heating 60 s, the bottom temperature by a constant  $k$  rises slower than that by a function  $k(T)$ . However, when the heating time exceeds 120 s, the bottom temperature by a function  $k(T)$  begins to exceed that by a constant  $k$ .

Using parameters given in tab 1, we can obtain the thermal behavior of C/C composites plate by the written code. Figure 3 displays the bottom temperature of C/C composites plate at different heating times. Within the initial heating 60 s, the bottom temperature by a constant  $k$  rises slower than that by a function  $k(T)$ . However, when the heating time exceeds 120 s, the bottom temperature by a function  $k(T)$  begins to exceed that by a constant  $k$ .

Using parameters given in tab 1, we can obtain the thermal behavior of C/C composites plate by the written code. Figure 3 displays the bottom temperature of C/C composites plate at different heating times. Within the initial heating 60 s, the bottom temperature by a constant  $k$  rises slower than that by a function  $k(T)$ . However, when the heating time exceeds 120 s, the bottom temperature by a function  $k(T)$  begins to exceed that by a constant  $k$ .

Using parameters given in tab 1, we can obtain the thermal behavior of C/C composites plate by the written code. Figure 3 displays the bottom temperature of C/C composites plate at different heating times. Within the initial heating 60 s, the bottom temperature by a constant  $k$  rises slower than that by a function  $k(T)$ . However, when the heating time exceeds 120 s, the bottom temperature by a function  $k(T)$  begins to exceed that by a constant  $k$ .

Using parameters given in tab 1, we can obtain the thermal behavior of C/C composites plate by the written code. Figure 3 displays the bottom temperature of C/C composites plate at different heating times. Within the initial heating 60 s, the bottom temperature by a constant  $k$  rises slower than that by a function  $k(T)$ . However, when the heating time exceeds 120 s, the bottom temperature by a function  $k(T)$  begins to exceed that by a constant  $k$ .

Using parameters given in tab 1, we can obtain the thermal behavior of C/C composites plate by the written code. Figure 3 displays the bottom temperature of C/C composites plate at different heating times. Within the initial heating 60 s, the bottom temperature by a constant  $k$  rises slower than that by a function  $k(T)$ . However, when the heating time exceeds 120 s, the bottom temperature by a function  $k(T)$  begins to exceed that by a constant  $k$ .

Using parameters given in tab 1, we can obtain the thermal behavior of C/C composites plate by the written code. Figure 3 displays the bottom temperature of C/C composites plate at different heating times. Within the initial heating 60 s, the bottom temperature by a constant  $k$  rises slower than that by a function  $k(T)$ . However, when the heating time exceeds 120 s, the bottom temperature by a function  $k(T)$  begins to exceed that by a constant  $k$ .

Using parameters given in tab 1, we can obtain the thermal behavior of C/C composites plate by the written code. Figure 3 displays the bottom temperature of C/C composites plate at different heating times. Within the initial heating 60 s, the bottom temperature by a constant  $k$  rises slower than that by a function  $k(T)$ . However, when the heating time exceeds 120 s, the bottom temperature by a function  $k(T)$  begins to exceed that by a constant  $k$ .

Using parameters given in tab 1, we can obtain the thermal behavior of C/C composites plate by the written code. Figure 3 displays the bottom temperature of C/C composites plate at different heating times. Within the initial heating 60 s, the bottom temperature by a constant  $k$  rises slower than that by a function  $k(T)$ . However, when the heating time exceeds 120 s, the bottom temperature by a function  $k(T)$  begins to exceed that by a constant  $k$ .

Using parameters given in tab 1, we can obtain the thermal behavior of C/C composites plate by the written code. Figure 3 displays the bottom temperature of C/C composites plate at different heating times. Within the initial heating 60 s, the bottom temperature by a constant  $k$  rises slower than that by a function  $k(T)$ . However, when the heating time exceeds 120 s, the bottom temperature by a function  $k(T)$  begins to exceed that by a constant  $k$ .

## Conclusions

Based on the Fourier's law of heat conduction and the computational scheme, we have obtained the effect of thermal conductivity on the ablation rate of a solid rocket nozzle. The results show that within the initial heating 60 s, both the bottom temperature and the ablative surface temperature by a constant  $k$  rise slower than that by a function  $k(T)$ . However, when the heating time exceeds 120 s, the bottom temperature by a function  $k(T)$  begins to exceed that by a constant  $k$ . In addition, the line ablation rate of C/C composites plate calculated by using actual thermal conductivity is higher than that by a constant thermal conductivity, so the effect of thermal conductivity on the ablation rate of a solid rocket nozzle made of C/C composites cannot be neglected.

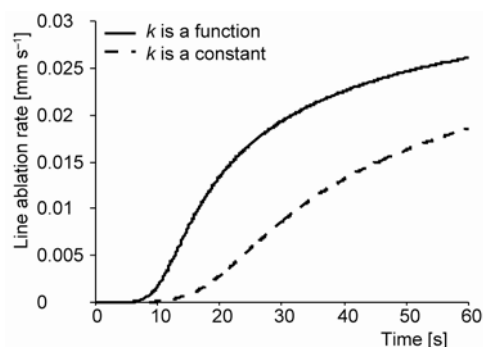


Figure 5. The line ablation rate of C/C composites plate vs. heating time

## Acknowledgments

This work was supported by the National Natural Sciences Foundation of China (11272042).

## Nomenclature

$c$  – specific heat capacity, [ $\text{Jkg}^{-1}\text{K}^{-1}$ ]  
 $h$  – enthalpy, [ $\text{MJkg}^{-1}$ ]  
 $k$  – thermal conductivity, [ $\text{Wm}^{-1}\text{K}^{-1}$ ]  
 $M$  – relative molecular weight, [-]  
 $\dot{m}_c$  – mass ablation rate, [ $\text{kgm}^{-2}\text{s}^{-1}$ ]  
 $q$  – heat flux on the surface, [ $\text{Wm}^{-2}$ ]

$s$  – ablation thickness, [mm]  
 $T$  – temperature, [K]  
 $v$  – line ablation rate, [ $\text{mms}^{-1}$ ]

### Greeks symbols

$\rho$  – density, [ $\text{kgm}^{-3}$ ]

## References

- [1] Lachaud, J., *et al.*, Analytical Modeling of the Steady State Ablation of a 3D C/C Composites, *International Journal of Heat and Mass Transfer*, 51 (2008), 9, pp. 2614-2627
- [2] Huang, H. M., *et al.*, Discrimination for Ablative Control Mechanism in Solid-Propellant Rocket Nozzle, *Science in China Series E*, 52 (2009), 10, pp. 2911-2917
- [3] Huang, H. M., Xu, X. L., A Combined Model for the Gaseous Mixture past a Cylinder in Ablation Environment, *International Journal of Applied Mechanics*, 3 (2011), 1, pp. 187-201
- [4] Lin, W. S., Quasi-Steady Solutions for the Ablation of Charring Materials, *International Journal of Heat and Mass Transfer*, 50 (2007), 5, pp. 1196-1201
- [5] Hristov, J., Heat-Balance Integral to Fractional (Half-Time) Heat Diffusion Sub-Model, *Thermal Science*, 14 (2010), 2, pp. 291-316
- [6] Pestchanyi, S., *et al.*, Estimation of Carbon Fiber Composites as ITER Divertor Armour, *Journal of Nuclear Materials*, 329 (2004), 8, pp. 697-701
- [7] Yin, J., *et al.*, Ablation Properties of Carbon/Carbon Composites with Tungsten Carbide, *Applied Surface Science*, 255 (2009), 9, pp. 5036-5040
- [8] Huang, H. M., *et al.*, Thermal Response of Heat-Resistant Layer with Pyrolysis, *Thermal Science*, 16 (2012), 1, pp. 69-78
- [9] Huang, H. M., *et al.*, Non-linear Analysis for Thermal Conduction in Carbon/Carbon Composites with Ablation, *Acta Materiae Compositae Sinica*, 29 (2012), 1, pp. 49-53

Paper submitted: February 2, 2014

Paper revised: April 12, 2014

Paper accepted: July 12, 2014